DOSE DUE TO PRACTICAL NEUTRON ENERGY DISTRIBUTIONS INCIDENT ON CONCRETE SHIELDING WALLS

by
J. M. Wyckoff
National Bureau of Standards, Washington, D.C. 20234

and

A. B. Chilton
Nuclear Engineering Laboratory
University of Illinois, Urbana-Champaign, Illinois 61801

Abstract

In order to calculate the dose equivalent for persons on the far side of an ordinary concrete shielding wall from a plane parallel source of neutrons, published monoenergetic neutron data and practical neutron spectra have been folded together. Some interpolation of the monoenergetic neutron data, both in energy and slab thickness, was required to prepared the data for computation in steps of 50 g/cm^2. The result is a set of useful dose-equivalent data for walls as thick as 800 g/cm^2 used to shield particle accelerators producing neutrons up to 100 MeV in energy. A simple, empirically derived, analytical expression for the dose equivalent for walls of 50 to 800 g/cm^2 thickness is given with suitable constants for neutron spectra produced by more than 60 selected examples of the following reactions: slow and fast neutron induced fission, (γ,n), (p,n), $(^3He,n)$, (α,n) and fission (γ,n).

Introduction

There is a famous recipe for rabbit stew that begins, "First you catch a rabbit." Many chefs never read beyond that first line. In a similar fashion, this brief paper must begin, "First you measure (or calculate) the total number of neutrons incident on each unit of area of an ordinary concrete shielding wall surrounding a neutron source, such as an accelerator." The material presented here allows a calculation of the tissue dose-equivalent, due to both neutrons and gamma rays induced in the shield at the far side of a wall of thickness z (in g/cm^2).

This calculation was undertaken to provide data in a readily usable form for shielding designers. The need for such information became evident in the preparation of design guidelines for accelerator facilities by Scientific Committee #22 of the National Council on Radiation Protection and Measurement, and the results will be used in that document. Multi-collision dose-equivalent due to monoenergetic plane-parallel neutrons incident on ordinary concrete walls has been reported by Roussin and Schmidt[1] (herein after called R&S), R.G. Alsmiller et al[2] (herein after called AMBE) and by Roussin, Alsmiller and Barish[3] (herein after called RAB) for neutron energies from thermal up to 400 MeV. Also, a large member of workers have measured neutron energy spectra and reported their results. A good-sized sample of these spectra, representative of thick target conditions, in the vicinity of 1 to 100 MeV particle accelerators have been taken from the literature. This report gives the results of a straight forward folding of some of these two types of data together.

There are several factors, not discussed in this report, which also influence the work of a neutron shielding designer. For the variation of energy spectra and neutron flux with angle, we refer the reader to many of the articles given as references for the neutron energy spectra. A recent study by one of the authors[4] (ABC) has shown the importance of water content and other constituents on shielding for neutrons up to 15 MeV in energy. In this report, only a single silicacious type of concrete is considered with a density of 2.31 g/cm^2 and composition as used by R&S and by RAB in units of 10^{21} atoms per cubic centimeter as follows: H(8.5), C(20.50), O(35.50), Mg(1.86), Al(0.60), Si(1.70), Ca(11.30) and Fe(0.19). This concrete has 5.5% water, by weight. The location of any type of ducts or irregularities in the wall has a strong bearing on neutrons shielding characteristics and has been discussed in detail elsewhere[5].

It should be noted that dose-equivalent is a defined quantity without direct physical significance. Neutron energy and gamma-ray energy are physical quantities, but the quality factor which relates these quantities to dose equivalent is the result of biological investigations. The set of fluence-to-dose-equivalent conversion factors used by R&S, AMBE and RAB is given in reference 1 and are consistent with the information given in NCRP Report No. 38[6].

This report is organized in 4 sections. The first discusses the neutron energy spectra selected from the literature for the calculations. The second presents the monoenergetic neutron dose equivalent data derived from R&S, AMBE and RAB. The third section discusses the dose equivalent calculations including an empirical analytical fit to the resulting dose equivalent data. The forth and final section presents a few comments on the results obtained.

I. The Neutron Energy Spectra

To the extent that beam particle type, incident particle energy, target material and target geometry vary, the data taken from the literature can only be considered to be a fair sample of the neutron spectra to be expected under other circumstances. The spectra used are listed in Table 1 where part (a) includes 3 fission cases[7] and 3 (α,n) cases[8]; part (b) includes 35 (p,n) spectra and a single $(^3He,n)$ case and part (c) includes 20 bremsstrahlung induced (γ,n) spectra for a total of 62 spectra. In some cases neutron energy spectra are integrated over all angles, but most of these data are for neutrons leaving a target in a restricted angular region. The constants A, B, and C listed in these tables relate to the empirical dose equivalent expression to be discussed in section III. As the format and scale of the original

Table 1
Neutron Sources and Related Dose Equivalent Constants

Table 1a No.	Incident Particle	Particle Source	Particle Target	A	B	C	Ref. No.
1	α	Ra	Be	.1611	.3697	.4318	7
2	α	Po	Be	.1618	.3624	.3458	7
3	α	Pu	Be	.1620	.3593	.3025	7
4	n(slow)	fission	^{235}U	.1658	.3857	.7290	7
5	n th	fission	^{235}U	.1629	.3824	.6543	8
6	n fast	fission	^{235}U	.1632	.3506	.1990	8

Table 1b No.	Proton Energy	Proton Target	n angle to beam	A	B	C	Ref. No.
1	8	C	0	.1615	.4096	1.031	8
2	9	C	0	.1609	.3686	.3913	8
3	11	C	0	.1610	.3956	.8178	8
4	12	C	0	.1609	.3926	.7700	8
5	13	C	0	.1614	.3910	.7502	8
6	11	C	90	.1606	.4172	1.181	8
7	12	C	90	.1628	.4087	1.057	8
8	11	H_2O	90	.1668	.4252	1.378	8
9	12	H_2O	90	.1667	.4052	1.036	8
10	13	H_2O	90	.1661	.4078	1.074	8
11	10	Mg	0	.1653	.4234	1.333	8
12	11	Mg	0	.1643	.4140	1.161	8
13	12	Mg	0	.1640	.4090	1.074	8
14	14.0	Al	10	.1631	.3441	.1323	9
15	15.7	Al	10	.1620	.3396	.06872	9
16	16.3	Al	10	.1621	.3401	.07353	9
17	16.5	Al	10	.1625	.3400	.07496	9
18	18.0	Al	10	.1620	.3392	.06556	9
19	18.5	Al	10	.1632	.3415	.09840	9
20	20	Al	10	.1624	.3397	.07029	9
21	10	Si	0	.1623	.4265	1.371	8
22	11	Si	0	.1632	.4140	1.140	8
23	12	Si	0	.1635	.4120	1.111	8
24	10	S	0	.1664	.4256	1.391	8
25	11	S	0	.1696	.4256	1.439	8
26	12	S	0	.1680	.4243	1.389	8
27	8	Ta	0	.1708	.4285	1.501	8
28	9	Ta	0	.1706	.4270	1.468	8
29	10	Ta	0	.1704	.4253	1.433	8
30	11	Ta	0	.1711	.4211	1.367	8
31	12	Ta	0	.1705	.4207	1.348	8
32	13	Ta	0	.1701	.4206	1.343	8
33	11	Ta	90	.1716	.4250	1.443	8
34	12	Ta	90	.1702	.4253	1.434	8
35	13	Ta	90	.1708	.4224	1.383	8

Table 1b No.	^3He Energy	^3He Target	n angle to beam	A	B	C	Ref. No.
36	18	Cu		.1630	.3780	.5881	14

Table 1c No.	Brems. Energy	Brems. Target	angle to beam	A	B	C	Ref. No.
1	16	Pt	90	.1722	.4222	1.397	10
2	16	Pb	90	.1660	.4184	1.256	10
3	13	Bi	90	.1680	.4212	1.325	10
4	16	U	90	.1704	.4090	1.141	10
5	34	^{16}O	55	.1619	.3428	.09096	11
6	34	^{16}O	93	.1615	.3462	.1279	11
7	34	^{16}O	141	.1622	.3488	.1669	11
8	45	^{238}U	90	.1646	.3893	.7646	8
9	55	Be	67.5	.1575	.2374	.2266	12
10	55	Pb	67.5	.1585	.2697	1.207	12
11	65	^{12}C	90	.1601	.2979	.2126	13
12	65	^{16}O	90	.1600	.3145	.2923	13
13	65	^{24}Mg	90	.1606	.2866	.1543	13
14	65	^{27}Al	90	.1608	.2845	.1446	13
15	65	^{28}Si	90	.1596	.2942	.1717	13
16	65	^{40}Ca	90	.1609	.2904	.1864	13
17	65	^{59}Co	90	.1595	.3217	.2675	13
18	65	^{181}Ta	90	.1607	.3185	.3681	13
19	85	Be	67.5	.1601	.1941	.4703	12
20	85	Pb	67.5	.1582	.2506	.4734	12

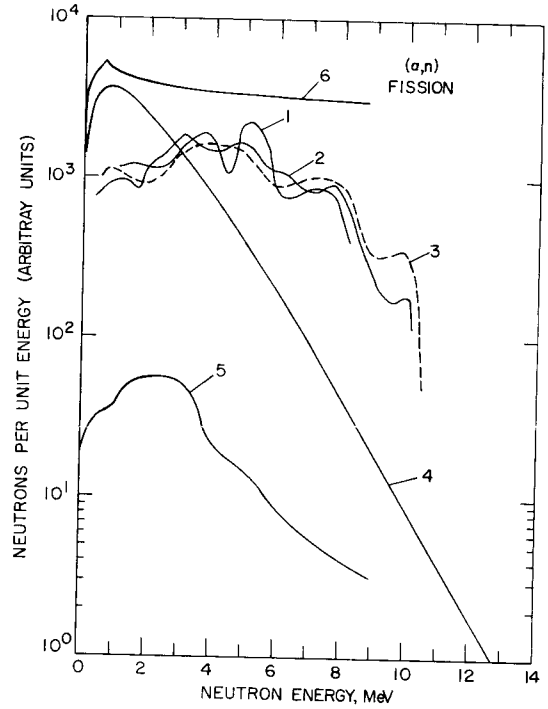

Figure 1

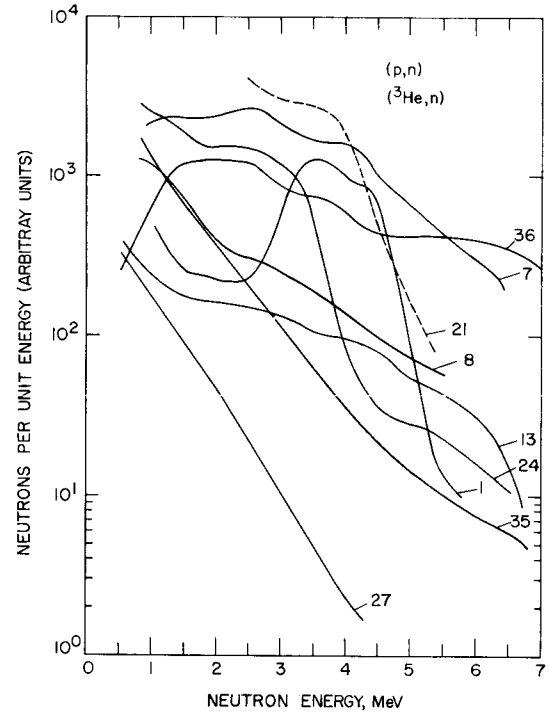

Figure 2

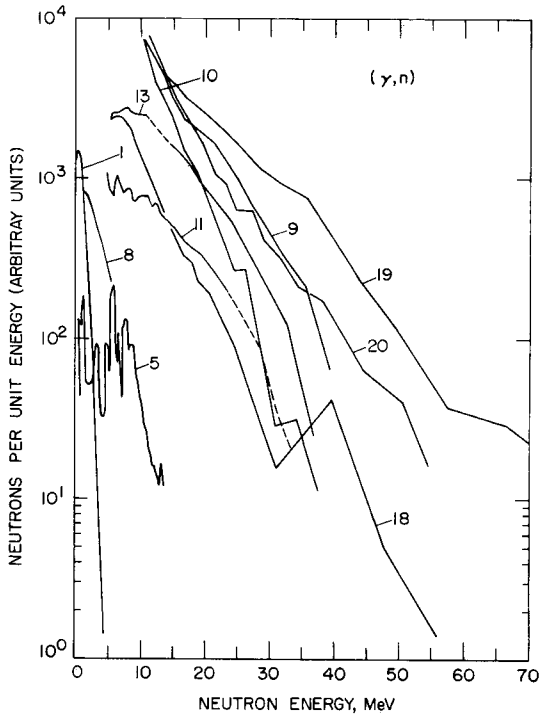

Figure 3

CAPTIONS

1. Neutron spectra from beryllium bombarded by α particles in (1) Ra-Be (2) Po-Be and (3) Pu-Be sources, and fission spectra from a (4) ^{235}U, (5) a thermal reactor core and (6) a faster reactor core. Note that the faster reactor data is incomplete on the high energy side.

2. Neutron spectra produced by proton bombardment of a number of targets obtained at angles to the beam indicated in parenthesis: 1. 8 MeV C(0°), 7. 12 MeV C(90°), 8. 11 MeV H_2O (90°), 13. 12 MeV Mg(0°), 19. 18.5 MeV Al((10°), 21. 10 MeV Si(0°), 24. 10 MeV S(0°), 27. 8 MeV Ta(0°), and 35. 13 MeV Ta(90°). The neutron spectrum produced by 18 MeV ^3He incident on Cu 11 is plotted in curve 36.

3. Neutron spectra produced by bremsstrahlung bombardment of the targets indicated with neutrons emerging at the angles indicated in parenthesis: 1. 16 MeV Pt(90°), 5. 34 MeV ^{16}O(55°), 8. 45 MeV ^{238}U(90°), 9. 55 MeV BE(67.5°), 10. 55 MeV Pb(67.5°), 11. 65 MeV ^{12}C(90°), 13. 65 MeV ^{24}Mg(90°), 19. 85 MeV Be(67.5°), and 20. 85 MeV Pb(67.5°).

drawings varies widely, selected samples of these input data have been replotted in Figures 1, 2, and 3 on semi-log graphs so that shape differences and limitations on some of the data can be appreciated. The α source and fission spectra are included for completeness though of limited use in accelerator shielding situations.

II. The Monoenergetic Neutron Dose Equivalent Data

The data in Table 1 is the tissue dose equivalent per neutron due to both neutrons and the γ-rays produced in the shielding concrete for each of energy bins indicated. The original data used to prepared this table came from the three sources already mentioned[1-3]. Each had to be adapted to this application.

R&S[1] covered concrete-slab penetration by neutrons in 22 energy groups covering the energy range from thermal to 15 MeV and slab thicknesses to 642 g/cm^2. Similar data reported by one of the authors (ABC)[2] allowed extrapolation of this data to thicknesses of 800 g/cm^2. Interpolation in slab thickness was used to tabulate these data in steps of 50 g/cm^2.

RAB[3] extended the energy range by making calculations at 25, 50, and 75 MeV for slabs as thick as 1500 g/cm^2. AMBE[4] reported calculation for SiO_2 and 5% H_2O at 100 MeV. Since neutrons interact, at such high energies, largely with individual nucleons, calculations for such a simplified material may fairly be used for a concrete shield calculation. RAB confirmed this by means of a calculation at 50 MeV which showed little difference between a more realistic concrete composition and the SiO_2-H_2O model. The results of these two calculations of dose equivalent inside a shield were used to obtain dose-equivalent on the far side of a shielding wall. A correction to account for the droop in dose equivalent near the exit surface due to a lack of backscattering had to be made. This correction process is not precise so some uncertainty is introduced in the results by this step. Since the energies used in the dose equivalent matrix of this report are at 20, 32.5, 50, 70, and 100 MeV it was necessary to interpolate, not only with respect to thickness as was done in the case of the R&S data, but also with respect to incident energy.

Table 1 may be employed with any plane parallel incident neutron energy spectra to obtain the tissue dose equivalent on the far side of a concrete shielding wall.

III. Computation of the Dose Equivalent

The matrix multiplication used to fold the neutron spectra f(E) into the dose equivalent matrix R(Z,E) is

$$D(Z) = \sum_{i=1}^{i=27} f(E_i)\ R(Z, E_i)\ \Delta E_i$$

The results obtained for about one-third of the spectra are plotted in Figure 4 for values of Z ranging from 0 to 800 g/cm^2. Dose in this case is in units rem·cm^2·n^{-1}.

The dose equivalent when plotted on a semi-log plot tends toward a straight line at greater depth which suggested the possibility of an empirical fitting of the data by an equation of the form

$$\text{Ln } D(Z) = -A\cdot 10^{2} - B\cdot 10^{-1}\,\frac{Z}{Z_0} + C\cdot 10^{-5}\,\frac{Z}{Z_0}^{2}$$

where $Z_0 = 1$ g/cm^2.

Using this expression as a basis function, a polynomial least squares fit was made for the D(Z) data for each calculated case. It was found that a reasonable χ^2 could be obtained if the first and last data points were dropped so, for this case, the values are listed in table 1a, b, and c. Where values of D(Z) calculated by this approximation are compared to the original data differences of up to 18% are observed but the mean difference is considerably less. Since D(Z) varies by more than 10 decades for the walls considered, this fit, which corresponds to an uncertainty of about 10 g/cm^2, is impressively good in the region above 50 g/cm^2. Below 50 g/cm^2 errors up to a factor of 3 are possible.

Examination of the basis function makes it clear that the first term establishes an incident plane intercept, the second term determines the slope and the third term applies a small correction to the slope.

IV. Comments on the Results

The first generalization about the dose equivalent as a function of shielding wall thickness is that for three cases, neutrons produced by fission, by Be(α,n) processes and by (p,n) processes shielding thickness required is very similar. Variations of 25 g/cm^2 separate the extremes for (α,n) and fission processes. Variations of about 60 g/cm^2 separate the extremes for (p,n) processes. In sharp contrast to this, (γ,n) processes require shielding that is very much a function of energy. For example, a shielding wall adequate for a 16 MeV bremsstrahlung platinum target must be doubled in thickness for an 85 MeV brensstrahlung lead target producing an equal flux of neutrons at the entrance plane. The dose equivalent calculated for the neutrons produced by bremsstrahlung striking ^{238}U are an understandable exception due to the admixture of low energy fission neutrons produced.

Small changes in the energy of protons incident on the target material, and in the angle of exit of neutrons leaving the target material, seem to have only minimal effect on the shielding requirements.

There is a lack of data (known to these authors) on experimental determination of dose equivalent for cases involving the inevitable mixture of neutrons and x-rays leaving a thick concrete shield when higher energy neutrons are incident.

Acknowledgement

The authors are indebted to Gerard Cavanaugh and Theordore Kraft who did much of the data processing for this study. We also appreciate the encouragement from E. Alfred Burrill who showed a keen interest in these calculations as they developed.

TABLE 2

Monoenergetic Neutron Dose Equivalent

Increment No.	Energy Interval (MeV)		Z=0	Z=50	Z=100	Z=150	Z=200	Z=250	Z=300	Z=350	Z=400
1	0.	4.14E-07	0.10E-08	0.18E-09	0.30E-10	0.51E-11	0.99E-12	0.21E-12	0.46E-13	0.11E-13	0.30E-14
2	4.14E-07	1.12E-06	0.12E-08	0.31E-09	0.48E-10	0.81E-11	0.16E-11	0.33E-12	0.74E-13	0.17E-13	0.42E-14
3	1.12E-06	3.06E-06	0.12E-08	0.35E-09	0.55E-10	0.93E-11	0.18E-11	0.38E-12	0.84E-13	0.20E-13	0.48E-14
4	3.06E-06	1.07E-05	0.12E-08	0.38E-09	0.62E-10	0.11E-10	0.20E-11	0.40E-12	0.92E-13	0.21E-13	0.52E-14
5	1.07E-05	2.90E-05	0.13E-08	0.40E-09	0.66E-10	0.12E-10	0.21E-11	0.43E-12	0.98E-13	0.23E-13	0.55E-14
6	2.90E-05	1.01E-04	0.13E-08	0.42E-09	0.73E-10	0.12E-10	0.23E-11	0.44E-12	0.99E-13	0.24E-13	0.58E-14
7	1.01E-04	5.83E-04	0.13E-08	0.43E-09	0.77E-10	0.13E-10	0.24E-11	0.46E-12	0.10E-12	0.25E-13	0.60E-14
8	5.83E-04	3.35E-03	0.12E-08	0.44E-09	0.81E-10	0.14E-10	0.25E-11	0.50E-12	0.11E-12	0.26E-13	0.63E-14
9	3.35E-03	1.11E-01	0.35E-08	0.44E-09	0.80E-10	0.14E-10	0.25E-11	0.50E-12	0.11E-12	0.25E-13	0.61E-14
10	1.11E-01	5.50E-01	0.16E-07	0.70E-09	0.97E-10	0.17E-10	0.30E-11	0.57E-12	0.13E-12	0.28E-13	0.68E-14
11	5.50E-01	1.11	0.31E-07	0.22E-08	0.19E-09	0.29E-10	0.49E-11	0.95E-12	0.20E-12	0.43E-13	0.92E-14
12	1.11	1.83	0.37E-07	0.64E-08	0.49E-09	0.59E-10	0.91E-11	0.17E-11	0.35E-12	0.74E-13	0.18E-13
13	1.83	2.35	0.36E-07	0.12E-07	0.12E-08	0.15E-09	0.19E-10	0.32E-11	0.49E-12	0.13E-12	0.29E-13
14	2.35	2.46	0.35E-07	0.16E-07	0.31E-08	0.46E-09	0.69E-10	0.10E-10	0.17E-11	0.31E-12	0.65E-13
15	2.46	3.01	0.35E-07	0.14E-07	0.23E-08	0.32E-09	0.43E-10	0.63E-11	0.11E-11	0.21E-12	0.44E-13
16	3.01	4.07	0.36E-07	0.13E-07	0.18E-08	0.24E-09	0.33E-10	0.50E-11	0.83E-12	0.16E-12	0.34E-13
17	4.07	4.97	0.37E-07	0.17E-07	0.32E-08	0.50E-09	0.73E-10	0.12E-10	0.18E-11	0.31E-12	0.61E-13
18	4.97	6.36	0.39E-07	0.17E-07	0.40E-08	0.78E-09	0.14E-09	0.23E-10	0.36E-11	0.63E-12	0.12E-12
19	6.36	8.19	0.41E-07	0.17E-07	0.42E-08	0.84E-09	0.16E-09	0.29E-10	0.53E-11	0.89E-12	0.17E-12
20	8.19	10.0	0.42E-07	0.18E-07	0.43E-08	0.89E-09	0.17E-09	0.32E-10	0.59E-11	0.11E-11	0.20E-12
21	10.0	12.2	0.46E-07	0.18E-07	0.43E-08	0.85E-09	0.16E-09	0.28E-10	0.50E-11	0.87E-12	0.17E-12
22	12.2	15.0	0.56E-07	0.21E-07	0.50E-08	0.11E-08	0.20E-09	0.39E-10	0.70E-11	0.13E-11	0.24E-12
23	15.0	25.0	0.62E-07	0.57E-07	0.19E-07	0.56E-08	0.14E-08	0.30E-09	0.60E-10	0.13E-10	0.31E-11
24	25.0	40.0	0.70E-07	0.62E-07	0.31E-07	0.13E-07	0.46E-08	0.14E-08	0.48E-09	0.15E-09	0.42E-10
25	40.0	60.0	0.67E-07	0.62E-07	0.37E-07	0.20E-07	0.10E-07	0.45E-08	0.19E-08	0.82E-09	0.34E-09
26	60.0	80.0	0.59E-07	0.64E-07	0.44E-07	0.26E-07	0.16E-07	0.82E-08	0.43E-08	0.23E-08	0.12E-08
27	80.0	120.0	0.50E-07	0.60E-07	0.46E-07	0.33E-07	0.22E-07	0.14E-07	0.85E-08	0.52E-08	0.31E-08

			Z=450	Z=500	Z=550	Z=600	Z=650	Z=700	Z=750	Z=800
1	0.	4.14E-07	0.80E-15	0.23E-15	0.65E-16	0.18E-16	0.	0.	0.	0.
2	4.14E-07	1.12E-06	0.11E-14	0.26E-15	0.67E-16	0.17E-16	0.	0.	0.	0.
3	1.12E-06	3.06E-06	0.12E-14	0.30E-15	0.76E-16	0.19E-16	0.	0.	0.	0.
4	3.06E-06	1.07E-05	0.13E-14	0.32E-15	0.80E-16	0.20E-16	0.	0.	0.	0.
5	1.07E-05	2.90E-05	0.14E-14	0.33E-15	0.84E-16	0.21E-16	0.	0.	0.	0.
6	2.90E-05	1.01E-04	0.15E-14	0.36E-15	0.88E-16	0.21E-16	0.	0.	0.	0.
7	1.01E-04	5.83E-04	0.15E-14	0.37E-15	0.91E-16	0.22E-16	0.	0.	0.	0.
8	5.83E-04	3.35E-03	0.16E-14	0.38E-15	0.94E-16	0.23E-16	0.	0.	0.	0.
9	3.35E-03	1.11E-01	0.15E-14	0.36E-15	0.85E-16	0.20E-16	0.	0.	0.	0.
10	1.11E-01	5.50E-01	0.17E-14	0.40E-15	0.97E-16	0.23E-16	0.	0.	0.	0.
11	5.50E-01	1.11	0.20E-14	0.43E-15	0.94E-16	0.21E-16	0.	0.	0.	0.
12	1.11	1.83	0.42E-14	0.98E-15	0.24E-15	0.59E-16	0.14E-16	0.	0.	0.
13	1.83	2.35	0.67E-14	0.16E-14	0.36E-15	0.83E-16	0.19E-16	0.	0.	0.
14	2.35	2.46	0.14E-13	0.29E-14	0.60E-15	0.13E-15	0.28E-16	0.	0.	0.
15	2.46	3.01	0.97E-14	0.21E-14	0.46E-15	0.10E-15	0.22E-16	0.	0.	0.
16	3.01	4.07	0.75E-14	0.17E-14	0.36E-15	0.80E-16	0.18E-16	0.	0.	0.
17	4.07	4.97	0.12E-13	0.25E-14	0.50E-15	0.10E-15	0.19E-16	0.	0.	0.
18	4.97	6.36	0.22E-13	0.40E-14	0.74E-15	0.14E-15	0.26E-16	0.	0.	0.
19	6.36	8.19	0.31E-13	0.57E-14	0.11E-14	0.20E-15	0.38E-16	0.	0.	0.
20	8.19	10.0	0.37E-13	0.70E-14	0.13E-14	0.25E-15	0.48E-16	0.	0.	0.
21	10.0	12.2	0.32E-13	0.59E-14	0.12E-14	0.22E-15	0.43E-16	0.	0.	0.
22	12.2	15.0	0.46E-13	0.87E-14	0.17E-14	0.32E-15	0.61E-16	0.12E-16	0.	0.
23	15.0	25.0	0.58E-12	0.14E-12	0.28E-13	0.57E-14	0.13E-14	0.30E-15	0.67E-16	0.16E-16
24	25.0	40.0	0.12E-10	0.39E-11	0.11E-11	0.28E-12	0.75E-13	0.22E-13	0.48E-14	0.10E-14
25	40.0	60.0	0.14E-09	0.59E-10	0.24E-10	0.95E-11	0.37E-11	0.15E-11	0.53E-12	0.20E-12
26	60.0	80.0	0.60E-09	0.29E-09	0.15E-09	0.82E-10	0.36E-10	0.20E-10	0.92E-11	0.46E-11
27	80.0	120.0	0.19E-08	0.11E-08	0.64E-09	0.36E-09	0.21E-09	0.12E-09	0.65E-10	0.35E-10

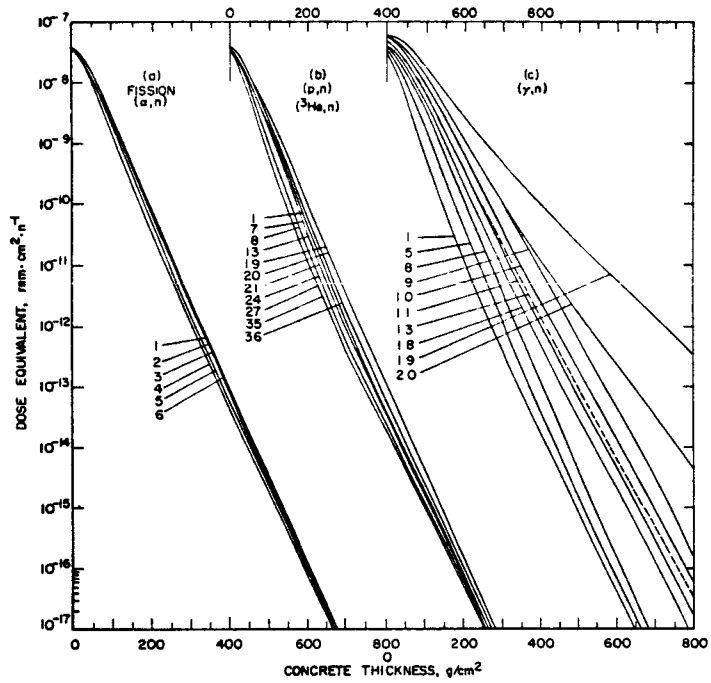

Figure 4. Tissue dose-equivalent at the far side of a concrete shielding wall for plane parallel incident neutron spectra. Fission process and α-beryllium sources indicated by number are listed in Table Ia and shown in (a). (p,n) and (^{3}He,n) data are shown in (b) and (γ,n) data is shown in (c). The concrete thickness axis has been shifted by 400 g/cm^2 for (b) and (c) in order to avoid confusion of closely spaced data.

REFERENCES

1. R.W. Roussin and F.A.R. Schmidt, "Adjoint S_n Calculations of Coupled Neutron and Gamma-Ray Transport Through Concrete Slabs," Nucl. Eng. and Des. 15, 3, 319 (1971).

2. R.G. Alsmiller, Jr., F.R. Mynatt, J. Barish and W.W. Engle, Jr., "Shielding Against Neutrons in the Energy Range 50 to 400 MeV," Nucl. Instr. and Meth. 72 213 (1969) (Also published as ORNL-TM-2554).

3. R.W. Roussin, R.G. Alsmiller, Jr. and J. Barish, "Calculations of the Transport of Neutrons and Secondary Gamma-Rays Through Concrete for Incident neutrons in the Energy Range 15 to 75 MeV," Nucl. Eng. and Des. 24, 2 (1973).

4. Private Communication, A.B. Chilton, "Effect of Material Composition on Neutron Penetration of Concrete Slabs," Nat. Bur. Stds. Rpt. 10425, June 1971 (unpublished).

5. R.G. Jaeger, Editor, Engineering Compendium on Radiation Shielding Vol. 1, Shielding Fundamentals and Methods (Chapter 8) Springer-Verlag, New York (1970).

6. National Committee on Radiation Protection and Measurement, "Protection Against Neutron Radiation," NCRP Report No. 30 NCRP Wash (1970).

7. B.T. Price, C.C. Horton, and K.T. Spinney, "Radiation Shielding" Permagon Press, New York (1957) p. 146, 151.

8. International Commission on Radiation Units "Neutron Fluence, Neutrons Spectra and Kerma" ICRU Report 13 (1969).

9. G.R. Holeman, D.M. Shaw and K.W. Price, "Stray Neutron Spectra and Comparisen of Measurements with Discrete Ordinate Calculations" Proc. of the Second International Conference on Accelerator Dosimetry and Experience, CONF 691101 USAEC Div. of Tech. Info., Stanford (1969) p. 552.

10. Y.Y. Glazunov, M.V. Savin, I.N. Safina, E.F. Formuskin and Y.A. Khokhlov. "Photoneutron Spectra of Platinum, Bismuth, Lead and Uranium," Soviet Physics, JETP 19, 1284 (1964).

11. V.V. Verbinski and J.C. Courtney, "Photoneutron Spectra and Cross Sections for ^{12}C and ^{16}O," Nuclear Physics, 73 398 (1965).

12. N.N. Kaushal, E.J. Winhold, P.F. Yergin, H.A. Medicus and R.H. Augustson, "Fast Photoneutron Spectra Due to 50-85 MeV Photons," Phys. Rev. 175 1330 (1968).

13. F.W.K. Firk, "Energy Spectra of Photoneutrons at Excitation Energies up to 60 MeV," Proc, of the International Nuclear Physics Conf., Gatlinburg, Tenessee 852 (1966): Academic Press, New York and London (1967).

14. J.B. McCaslin and A.R. Smith, "Radiation Measurements and Shielding Study of the Berkeley, 27-inch ^{3}He Cyclotron," Proc. of the Second International Conference on Accelerator Dosimetry and Experience, CONF. 691101 USAEC Div. of Tech. Info., Stanford (1969) p. 486.